*Annals of Botany* **112**: 267–276, 2013
doi:10.1093/aob/mct047, available online at www.aob.oxfordjournals.org

ANNALS OF BOTANY
Founded 1887

TECHNICAL ARTICLE: PART OF A SPECIAL ISSUE ON MATCHING ROOTS TO THEIR ENVIRONMENT

# Quantitative imaging of rhizosphere pH and $CO_2$ dynamics with planar optodes

**Stephan Blossfeld[1,†]*, Christina Maria Schreiber[2,†], Gregor Liebsch[3], Arnd Jürgen Kuhn[1] and Philippe Hinsinger[2]**

[1]*Forschungszentrum Jülich GmbH, Institute of Bio- and Geosciences, IBG-2: Plant sciences, Jülich, Germany,* [2]*INRA, UMR Eco&Sols, Montpellier, France and* [3]*PreSens, Precision Sensing GmbH, Regensburg, Germany*
[†]*These authors contributed equally to this paper.*
* *For correspondence. E-mail s.blossfeld@fz-juelich.de*

Received: 2 October 2012 Revision requested: 7 November 2012 Accepted: 16 January 2013 Published electronically: 26 March 2013

• *Background and Aims* Live imaging methods have become extremely important for the exploration of biological processes. In particular, non-invasive measurement techniques are key to unravelling organism–environment interactions in close-to-natural set-ups, e.g. in the highly heterogeneous and difficult-to-probe environment of plant roots: the rhizosphere. pH and $CO_2$ concentration are the main drivers of rhizosphere processes. Being able to monitor these parameters at high spatio-temporal resolution is of utmost importance for relevant interpretation of the underlying processes, especially in the complex environment of non-sterile plant–soil systems. This study introduces the application of easy-to-use planar optode systems in different set-ups to quantify plant root–soil interactions.
• *Methods* pH- and recently developed $CO_2$-sensors were applied to rhizobox systems to investigate roots with different functional traits, highlighting the potential of these tools. Continuous and highly resolved real-time measurements were made of the pH dynamics around *Triticum turgidum durum* (durum wheat) roots, *Cicer arietinum* (chickpea) roots and nodules, and $CO_2$ dynamics in the rhizosphere of *Viminaria juncea*.
• *Key Results* Wheat root tips acidified slightly, while their root hair zone alkalized their rhizosphere by more than 1 pH unit and the effect of irrigation on soil pH could be visualized as well. Chickpea roots and nodules acidified the surrounding soil during $N_2$ fixation and showed diurnal changes in acidification activity. A growing root of *V. juncea* exhibited a large zone of influence (mm) on soil $CO_2$ content and therefore on its biogeochemical surrounding, all contributing to the extreme complexity of the root–soil interactions.
• *Conclusions* This technique provides a unique tool for future root research applications and overcomes limitations of previous systems by creating quantitative maps without, for example, interpolation and time delays between single data points.

**Key words:** *Triticum turgidum durum*, *Cicer arietinum*, *Viminaria juncea*, planar optodes, rhizosphere, quantitative imaging, pH dynamics, $CO_2$ dynamics.

## INTRODUCTION

The rhizosphere is defined as the volume of soil that is affected by root activities (Hiltner, 1904). However, assessment and understanding of this simple and clearly defined environmental hot spot is not trivial, especially when it comes to the level of biogeochemical process analysis (Hinsinger *et al.*, 2005). A prerequisite for a detailed understanding of plant root – rhizosphere – bulk soil interactions is knowledge of the spatial and temporal dynamics of pH, $O_2$ and $CO_2$ partial pressure ($pCO_2$). These key factors provide the framework for all biogeochemical processes and are indeed of great ecological relevance for ecosystem functioning (Hinsinger *et al.*, 2009).

Successful elucidation of biogeochemical processes in the rhizosphere is strongly dependent on the available methods and technologies for assessing and monitoring the spatial and temporal dynamics of pH, $O_2$ and $CO_2$ without disturbing the original processes (Neumann *et al.*, 2009). Planar optodes are the present state-of-the-art technology for this purpose. They allow a detailed non-invasive quantitative imaging of the dynamics of protons, molecular oxygen and even carbon dioxide in the rhizosphere. Recent findings have described the dynamics of protons or molecular oxygen in the rhizosphere, monitored by means of quantitative imaging systems at medium to high spatial and temporal resolution (Blossfeld and Gansert, 2007; Blossfeld *et al.*, 2011; Rudolph *et al.*, 2012; Schreiber *et al.*, 2012). These are among the few reports on spatial and temporal patterns of rhizosphere development at the relevant scales for understanding root-mediated processes. However, rhizosphere optode measurements were mostly made using fibre optic systems. Although being highly precise in terms of analyte concentration determination and temporal resolution, this approach only provides data from a grid of measurement spots (at best 1·5 × 1·5 mm; Schreiber *et al.*, 2012). Such discrete data have then to be interpolated to obtain a quantitative picture. Data interpolation is not necessary to produce high-resolution images from the novel device described in the present work. The false colour images produced need no further processing and can be immediately used for visualization of the spatial pattern of, for example, pH over time.

Needle-type sensors offer the same precise measurement with a 20-μm tip, which is highly useful in confined spaces (vessels etc.), but cannot provide non-invasive measurements

over large areas. Furthermore, most of these systems require a rather sophisticated set-up, and generally the required analytical software needs to be developed specifically (Blossfeld and Gansert, 2007; Blossfeld *et al.*, 2011; Rudolph *et al.*, 2012).

Thus, the distribution and use of this technology is rather limited, and hence the limited number of references so far. Watt *et al.* (2006) and Walter *et al.* (2009) recently stressed the need to further our rather poor understanding of rhizosphere development in space and time, which contrasts with the extensive advances made on 'bulk' rhizosphere biogeochemistry (Hinsinger *et al.*, 2009). For $CO_2$, to our knowledge, only one report can be found in the literature on the spatial distribution of $pCO_2$ in the rhizosphere (Gollany *et al.*, 1993), and none on its temporal dynamics, in spite of the importance of root and rhizosphere respiration to the global carbon cycle.

This technical report demonstrates a novel and easy-to-use quantitative imaging system that allows the monitoring of rhizosphere pH and $CO_2$ dynamics with planar optodes at high spatial and temporal resolution without being sophisticated in set-up or analytical software.

## MATERIAL AND METHODS

The novel system requires only minimal technical equipment but remains open to various user-defined extensions or adaptations. The system relies on a modified and easy-to-use USB-Microscope device and software (VisiSens; PreSens GmbH, Regensburg, Germany), as well as commercially available planar optodes. Besides the known planar optodes that are sensitive to pH (product code SF-HP5-OIW; PreSens GmbH), this system is also usable with $CO_2$ sensor foils (product code SF-CD1-US; PreSens GmbH).

The compact one-piece fluorescence microscope used in this study was especially designed for reading-out the signals of the pH and $CO_2$ sensor foils: an appropriate LED excitation light source, optical filters, lens and the camera chip are assembled in an aluminium housing 10 cm in length and 3·5 cm in diameter. The microscope is connected via USB2.0 to a PC-unit (e.g. a notebook), which makes it versatile and portable. The USB-microscope device delivers 24-bit, 1280 × 1024 (1·3 megapixel) RGB images containing the raw sensor response. In this study we used a distance of 20 or 60 mm between planar optodes and camera, which resulted in a field of view of 15 × 12mm or 45 × 36mm, and a pixel resolution of 10 or 20 μm, where every pixel carries discrete quantitative analyte information. The field of view determines the part of the picture which is interpretable and is not dependent on optode foil size, which can be smaller or greater. To measure planar optodes greater than the field of view, the camera has to be moved (e.g. via a step motor system as described in Blossfeld and Gansert, 2007) and the resulting images have to be arranged post-measurement. With the present set-up the best temporal resolution of measurement was one image every 2 s. However, adaptation to shutter and software could allow higher temporal resolution if needed. In this study we expected no quick changes of pH or $CO_2$ and therefore chose a 10-min time interval between the automated measurements. By doing so, a good relationship between temporal resolution and data quantity was achieved. A schematic overview of the camera system and set-up of the sensor can be found in Supplementary Data Fig. S1.

Imaging software (VisiSens AnalytiCal 1; PreSens GmbH) was then used to acquire the images of the pH and $pCO_2$ optodes and to compute the quantitative maps from the raw sensor response images. The results from pilot test runs with this novel system, performed under different environmental conditions and with different plant species, demonstrate the power of this system.

### *Principle of planar optodes*

The measuring principle of the planar optode technology has been described in detail in several articles (e.g. Holst and Grunwald, 2001; Gansert and Blossfeld, 2008). Thus, this report provides only a brief overview and we refer to the specialized literature for, for example, chemical details.

A planar optode represents a sensor foil with embedded fluorescent molecules, which emit a characteristic pattern (e.g. in terms of decay time or emission spectrum) of fluorescence after excitation depending on the analyte concentration. A camera that is sensitive within the emission range of the optode can be used to detect this fluorescence signal. Hence, the fluorescent light serves as the carrier of information. Furthermore, using light as information carrier allows separation of sensor (the planar optode) and detector (the camera). Consequently, non-invasive measurements in numerous set-ups are possible, i.e. the monitoring of rhizosphere processes in rhizobox set-ups or similar. Moreover, the use of a camera allows quantitative mapping of the analyte concentration over time.

Optode measurements in this study used the so-called ratiometric approach, which is based on the change of the emission spectrum of the planar optodes depending on the analyte concentration. In our case it is the ratio of red to green in the emitted fluorescence response which was recorded in the respective colour channels of an RGB colour CMOS chip. The optodes used consisted of analyte-sensitive and analyte-insensitive dyes (i.e. indicator and reference dye), which were simultaneously excited by the blue (470 nm) LEDs of the detector unit. The green fluorescence of the indicator dye is driven by the analyte with respect to its fluorescence intensity, whereas the red fluorescence of the reference is not affected. The colour RGB (red, green, blue) chip of the camera can capture the fluorescence signals in one single image and the subsequent data analysis by the software creates the ratio of the red and the green channel (i.e. R value), creating a two-dimensional map of the quantity of the measured parameter. A schematic overview of the processing of an RGB image can be found in the Supplementary Data Fig. S2.

A potential risk of signal interference by autofluorescence signals from roots or other material in the soil was avoided by the fact that the planar optode was not transparent and within the path of light, therefore absorbing the excitation light. Thus, no autofluorescence from material behind the planar optode could occur and alter our measurements.

For calibration purposes the sensor response was plotted against the respective analyte concentration. The corresponding pH or $CO_2$ concentration was calculated from this R

value by using a calibration function that was obtained with samples of known analyte concentration prior to the experiment (see below).

*Calibration procedures*

Calibration of the different planar optodes was done prior and after the experimental phase to rule out or take into account possible shifts in sensor response. Age and photobleaching can cause the sensor response to be altered, resulting in an altered recalibration curve. Earlier experiments with similar planar pH optodes, using a fibre-optic approach, have shown that this effect is rather low, e.g. 0·4 pH units after a long experimental period of 7 weeks in anoxic and reducing soils (Blossfeld and Gansert, 2007). In the present study no change of the sensor response was detectable after recalibration, mainly due to fact that the experimental periods were short (hours or days). As shown in the supplementary material, the precision of the pH measurement was excellent over a broad pH range, while there was a slight shift in the R value (corresponding to a maximum of 0·1 pH unit difference) occurring only for high pH values (Supplementary Data Fig. S3).

*Calibration procedure for the planar $CO_2$ optodes*

Due to the fact that the planar $CO_2$ optodes are sensing $CO_2$ partial pressure ($pCO_2$, i.e. the free $CO_2$ in the rhizosphere), the use of purified test gases of $CO_2$ to define calibration points is recommended. Hence, it should be stressed that assessment of the total $CO_2$ in the soil solution (including carbonate and bicarbonate) is of course only possible if the local pH and temperature are monitored as well (i.e. due to the mass action law and solubility of $CO_2$ at a given temperature). Note also that due to the measurement of $pCO_2$, the amount of moles of $CO_2$ can be different if measurements are performed in solution or in air. Here $CO_2$ was measured in solution only, due to the permanent waterlogging, and we did not investigate the carbonate and bicarbonate content.

For this particular pilot study we expected quite high $CO_2$ concentrations in the waterlogged substrate and therefore the calibration concentrations were: 0 vol. % (i.e. pure $N_2$ gas), 20 vol. %, 40 vol. %, 60 vol. % and 80 vol. %. For other studies, e.g. in non-waterlogged systems, a different calibration scheme with lower $CO_2$ concentrations is of course advisable to achieve an adequate precision of measurement. A replicate of the used planar $CO_2$ optodes (all from the same batch) was installed in a transparent Plexiglas container [i.e. calibration chamber of: 100 mm (width) × 100 mm (height) × 10 mm (depth), thickness of front plate 8 mm], which was half filled with deionized water. The solution of the calibration chamber was aerated with one of the gases for up to 10 min until the system was saturated and a constant R value was reached. During this time the R value of the planar optodes was monitored from outside the system every minute. This procedure was repeated for every concentration step. The resulting R values were used as input data of a Boltzmann fitting curve (Blossfeld and Gansert, 2007). The resulting fitting parameters were then used to calculate the $CO_2$ concentration. A demonstration of the precision of the $CO_2$ measurement depending on $CO_2$ range (maximum difference of 3·4 %) can be found in Supplementary Data Fig. S4.

*Calibration procedure for the planar pH optodes*

Two stock solutions of phosphate buffers with an ionic strength of 30 mM (solution A = 10 mM $KH_2PO_4$ + 20 mM NaCl and solution B = 10 mM $K_2HPO_4$) were used to produce the five calibration buffer solutions (pH 5, 6, 7, 8 and 9) by mixing different volumes of the stock solutions. Similar to the calibration of the planar $CO_2$ optodes, a replicate of the used planar pH optodes was installed in the calibration chamber. The calibration chamber was then filled with one of the pH buffer solutions, and the change of the R values of the planar optode was sensed from outside the system every minute over a period of 10 min and, by then the R value was constant. The resulting R values were used as input data of a Boltzmann fitting curve (Blossfeld and Gansert, 2007). The resulting fitting was then used to calculate the pH value.

*Experimental set-up*

*Example 1.* pH dynamics was monitored in the rhizosphere of durum wheat (*Triticum turgidum durum* 'LA1823') and chickpea (*Cicer arietinum* 'ILC 01302', inoculated with *Mesorhizobium ciceri* (UPM Ca7)), grown under greenhouse conditions (25 ± 2 °C, 8/16 h dark/light cycle, 50–55 % relative humidity).

Chickpea and wheat were both planted 2 weeks after germination into an individual well-sized rhizobox (84 × 34 × 2 cm) to enable almost uninhibited growth over several weeks. Additionally in another experiment, both species were planted together in a smaller rhizobox (40 × 20 × 2 cm) to enforce root interaction between the species. In this particular case, chickpea received no inoculation and the rhizobox was kept in a climate chamber (20 °C, 10/14 h dark/light cycle, 200 μmol photons $m^{-2}$ $s^{-1}$, 60 % relative humidity).

The transparent reverse side of the larger rhizoboxes contained 12 removable windows (six of 10 × 10 and six of 5 × 10 cm), offering permanent access to the root systems and soil and a choice of where to fit the optodes. The smaller rhizobox had a single front plate, which had to be removed to install the optode. Although it is possible to install the optode prior to planting, it is easier in a larger rhizobox to choose the points of interest during root growth (i.e. opening the rhizobox). This helps to avoid installing optodes in areas which are ultimately not colonized by roots, and it makes it possible to concentrate on points of interest. The use of small windows helps to minimize disturbance. After optode installation the rhizoboxes were tilted to 30° from the vertical and the camera was fixed 60 mm from the planar optode onto the rhizobox to monitor pH dynamics at 10-min intervals over the next few days (a shorter interval is also possible but results in larger data sets). The rhizoboxes were covered with lightproof material throughout the experiment to avoid light disturbances on root growth and sensor signal.

During plant growth, points of interest were chosen in the root systems, i.e. roots with root hairs (wheat) and $N_2$-fixing nodules (chickpea) or crossing over of roots of both species

to monitor the range, amplitude, and possible spatial and temporal dynamics of pH changes in the rhizosphere of these species. While chickpea as an $N_2$-fixing legume is expected to strongly acidify its rhizosphere, wheat is able to alkalize the rhizosphere depending on prevailing soil characteristics and nutrient supply (Marschner and Römheld, 1983; Raven *et al.*, 1990; Hinsinger *et al.*, 2003; Bravin *et al.*, 2009; Betencourt *et al.*, 2012).

In this example a Luvisol with clay-loam texture, neutral bulk soil pH, Olsen-P 30·4 mg $kg^{-1}$, $NO_3^-$ 20 mg $kg^{-1}$, $NH_4^+$ 0·56 mg $kg^{-1}$ and without additional fertilization was used. The N capture pathways ($N_2$ fixation vs. preferred $NO_3^-$ uptake against $OH^-$ ions) were expected to contribute strongly to visible pH dynamics, especially at points of higher metabolic activity (root tips, root hairs, nodules). The rhizobox was watered with 200 $cm^3$ of water daily (deionized water in greenhouse experiments, tap water in climate chamber experiments).

*Example 2.* Monitoring $CO_2$ dynamics in the rhizosphere of *Viminaria juncea*, grown in a climate chamber (20 °C, 10/14 h dark/light cycle, 200 µmol photons $m^{-2}$ $s^{-1}$, 60 % relative humidity).

*Viminaria juncea*, grown in a waterlogged sand-filled rhizobox (40 × 20 × 2 cm), was investigated for this short-term experiment. The quartz sand was rinsed with deionized water prior to transplantation of the seedling into the rhizobox. The rhizobox was kept waterlogged throughout the entire growth period by using a nutrient solution (50% Hoagland). It was decided to use waterlogged conditions to ensure high $CO_2$ partial pressures in the soil–rhizosphere interface (Greenway *et al.*, 2006), *V. juncea* being known to be well adapted to these conditions. The soil temperature was kept constant at 20 °C, to maintain equal respiration rates of roots and microorganisms throughout the experiment.

When the first roots reached the lower part of the rhizobox, it was opened and a planar $CO_2$ optode was placed onto the front plate of this rhizobox. The tip of a single root was just behind the upper corner of the planar optode when the plate was subsequently mounted on the rhizobox. A black spot made with a pen at the outer side of the front plate served as a mark for the initial position of the root tip. After closing the rhizobox, it was tilted at 30° from the vertical, forcing the root to grow just behind the planar optode. Then, the rhizobox was set to waterlogged conditions with nutrient solution again. After 1 d of equilibration, the camera was fixed onto the front plate of the rhizobox and the $CO_2$ content of the area behind this planar optode was measured at 10-min intervals over the next 3 d.

## RESULTS

*Example 1: monitoring pH dynamics in the rhizosphere of durum wheat (*Triticum turgidum durum*) and chickpea (*Cicer arietinum*)*

*(a) Two-day monitoring of the rhizosphere pH around growing wheat roots.* The maps show the pH rise around developing root hairs of growing wheat roots. Eight maps were taken from a time frame series (Fig. 1A–H). For a more detailed impression of the dynamics of this process please refer to the image sequence available in Supplementary Data Video S1. The pH in the bulk soil ranged from 6·8 to 7·2 (Fig. 1A, P1), while the

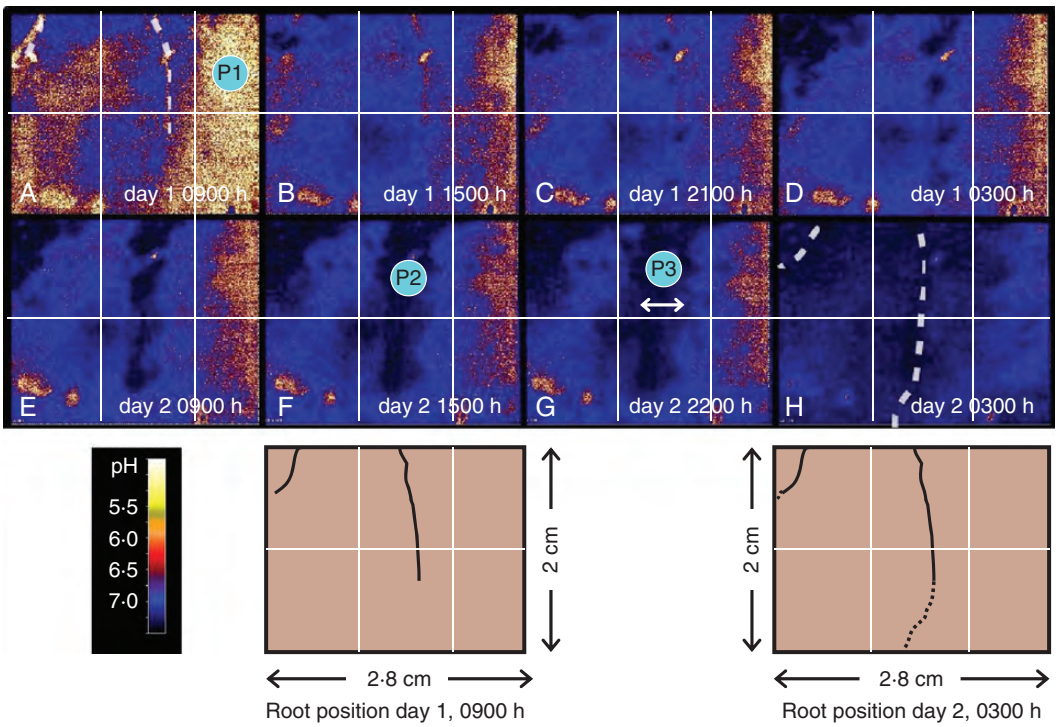


FIG. 1. (A–H) Maps of pH patterns around wheat roots, taken from a 48-h pH monitoring. White dotted lines and schematic drawings from the start and end of the experiment mark the position of roots. P1–3 mark points of interest (P1: bulk soil, P2: alkalization at root surface, P3: within alkalization zone). For additional images of pH dynamics we refer to the video sequences in Supplementary Data Video. S1.

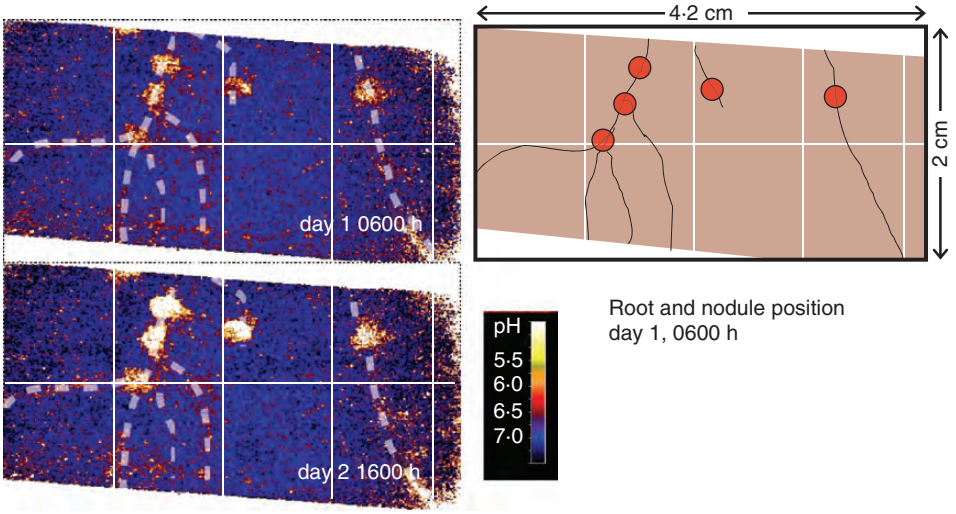


FIG. 2. The two pH maps display the lowest and highest pH values around chickpea nodules, taken from a 48-h pH monitoring. White dotted lines and schematic drawing mark the position of roots and nodules (red circles). For additional images of pH dynamics we refer to the video sequences in Supplementary Data Video S2.

wheat alkalized several millimetres around its roots up to pH 7·9 (Fig. 1F, P2). An influence zone of more than 5 mm from the roots was clearly visible (Fig. 1G, P3). Due to the activity of several roots, the whole measurement window was alkalized after 2 d (Fig. 1H).

*(b) Two-day monitoring of the rhizosphere pH in the vicinity of chickpea nodules.* The two maps in Fig. 2 show the lowest and highest amplitude of acidification around active chickpea nodules. During daytime (day 2 at 1600 h) the acidification around the nodules was stronger (pH 6·0) than during the night (pH 6·8 on day 1 at 0600 h), representing a diurnal rhythm of acidification. In contrast to the nodules, the roots themselves did not show such strong pH changes. The full animation of this pulsating pattern can be seen in Supplementary Data Video. S2. Nodules were considered active. Cutting them revealed red colouring due to the presence of leghaemoglobin (Ott *et al.*, 2005).

*(c) Ten-day monitoring of rhizosphere pH around intercropped wheat and chickpea roots.* Eight maps were taken from a time frame series (Fig. 3A–H, full animation available in Supplementary Data Video S3). The maps showed the pH change around developing lateral roots of chickpea (not inoculated with *Mesorhizobium ciceri*) and a growing wheat root. The black spots represent positioning marks made on the outside of the front plate of the rhizobox and therefore contain no pH signal.

The tip of the wheat root was growing across a chickpea root at the upper left area and the rhizosphere along the elongation zone was acidified from an initial pH of 8 to pH 7 (Fig. 3D, E, P1). This acidification stopped when the elongation zone passed by and root hairs were formed (Fig. 3F–H). It is clear that the initial pH of 8 was much higher than the bulk soil pH in experiment A (pH 6·8–7·2). This could be due to the different climates and watering regimes as well as due to the fact that the root system of this experiment C was very dense compared with that in experiment A, i.e. it cannot be ruled out that roots of wheat were hidden behind this particular soil area and therefore already influenced the soil pH.

The most prominent root of the mapped area was the chickpea root, which was growing from the top to the bottom at the centre of the maps (Fig. 3E, P2). Two lateral roots emerged from this root during the observation period. The main root and the basal parts of the lateral roots (Fig. 3B, P3, P4) acidified their rhizosphere strongly, down to pH 6 or even lower (i.e. 1–1·5 pH units), except for the area in the upper left corner where the wheat root crossed over the chickpea roots, which remained more alkaline. The tip of the upper lateral root showed a clearly localized zone of acidification (pH 6·2–6·5) that moved through the soil over time (Fig. 3G, P5). The central part of the planar optodes appeared as a horizontal acidic zone as well. This was actually due to some small cavities with entrapped air (i.e. not water filled) in the soil behind the optode (Fig. 4D). Without a contact to soil or roots, the sensor response is driven by the pH in the water film on the optode, which in turn depends on the local $pCO_2$ in the cavities and other neighbouring sources of protons in contact with this water film (i.e. the chickpea root in this case).

Interestingly, all roots displayed a diurnal pattern (Fig. 4A, B, E, F), which was closely linked to the time of the day (midday) when the rhizobox received the daily watering. As soon as the rhizobox was watered the pH of the investigated area increased rapidly. Depending on the particular location, the pH change was up to 0·5 pH units. After this quick change, the pH decreased down to the initial values again.

### *Example 2: three-day monitoring $CO_2$ dynamics in the rhizosphere of* Viminaria juncea

This series of six maps taken at a 12-h intervals (Fig. 5A–F) showed the fate of elevated $pCO_2$ in the rhizosphere of a growing root tip of *V. juncea*. The first map was obtained when the root tip was close to the blue circle in the upper right corner (i.e. a mark from outside the rhizobox). The

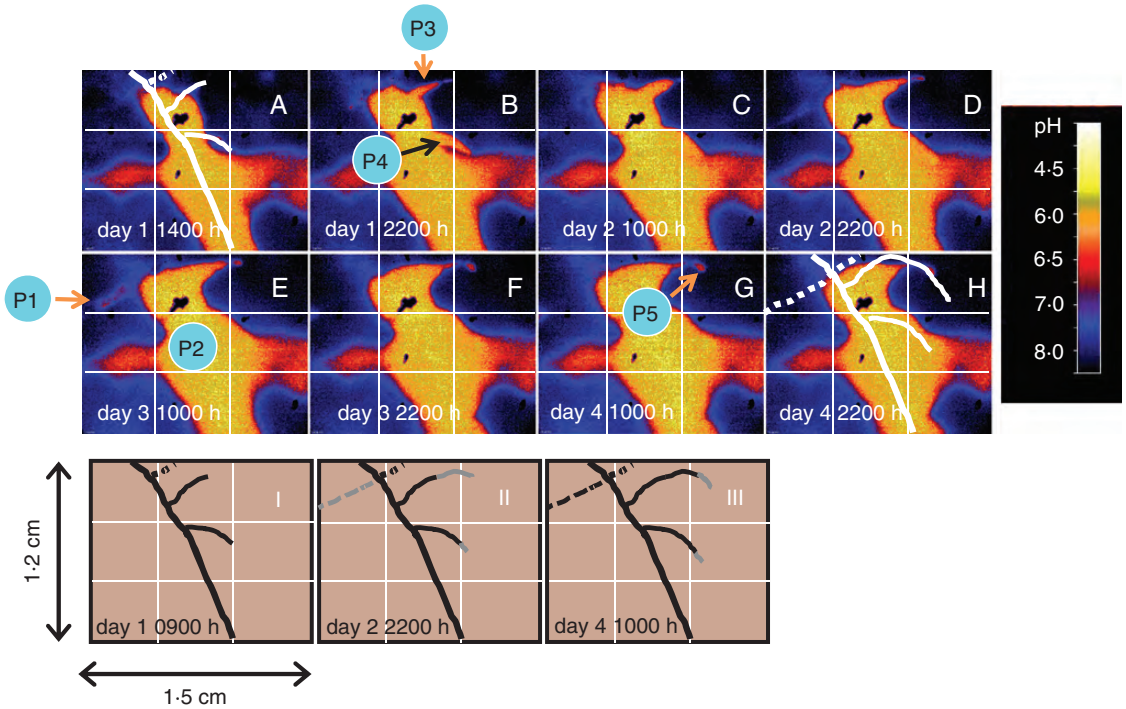


FIG. 3. (A–H) The eight pH maps display the dynamics of pH values around intercropped chickpea and wheat roots, taken from a 223-h pH monitoring (white labelling indicates day of the experiment and hours of the day). White lines mark the position of roots (solid = chickpea; dashed = wheat). I–III: estimated position of the roots behind planar optode during the course of the experiment; grey lines indicate root growth compared with day 1 of experiment. Key points are: elongation zone of wheat root (P1), chickpea root (P2), basal parts of lateral chickpea roots (P3, P4) and tip of lateral chickpea root (P5). For additional images of pH dynamics we refer to the video sequence in Supplementary Data Video S3.

following maps clearly showed that the $pCO_2$ rose along with the growing root. The $pCO_2$ rose from the top to the bottom, reaching values of up to 70 % of $CO_2$. The $pCO_2$ map in Fig. 5E corresponded to the time when the root tip had already left the investigated area. Due to $CO_2$ diffusion, the maps displayed an expanding and tapered-like $CO_2$ formation pattern until almost the entire investigated area reached a $pCO_2$ higher than 40 %. Only a small area in the upper left part of the investigated area showed a rather slow increase in $pCO_2$. The reason for this remained unclear to us. This phenomenon was probably due to a local microcavity with an entrapped air space, causing a delay in $CO_2$ enrichment. Full animation of the time series (covering the root growth over 3 d) can be seen in Supplementary Data Video S4.

## DISCUSSION

### *Assessment of the novel system*

This novel system proved to be a major step forward, as it makes it possible to generate quantitative maps of key rhizosphere parameters at high spatial resolution, without the need of interpolation of single data points as was done in previous studies (Blossfeld and Gansert, 2007; Blossfeld *et al.*, 2010, 2011; Schreiber *et al.*, 2012). For example, the latter technique would generate a single average pH value for an area of 7·07 $mm^2$ when using a spot diameter of 3 mm. By this, small areas with strong pH changes would have been overlooked, e.g. the acidic tips of lateral roots of chickpea (i.e. P5 in Fig. 3G). Hence, the previous techniques suffered from a loss of information and depending on the diameter of the single measuring spot and the size of the scanned planar optode a substantial time delay was actually occurring between the first and the last measuring spots.

When interpreting the quantitative maps derived from planar optodes, it is of course necessary to bear in mind that the soil properties, local inhomogeneity (e.g. air spaces) in the soil and activity of the plants (e.g. transpiration, root growth) might influence the diffusion and convection of the analytes and therefore the spatial pattern. Certainly, the measured concentration of, for example, protons at time point $x$ determines for the area that is behind each pixel, but the signal of the planar optodes does not include any information about the source, the diffusion vector, etc.

One drawback with regard to the use of planar optodes in general is that the position of the roots and the structure of the soil behind the planar optodes are not clearly visible. Hence, the position of roots during the course of the experiment has to be estimated according to the initial and final position at the end of the experiment.

Nevertheless, the optode sensor technique has become widely and effectively applied. As this system is fairly easy to handle and given the prospect of increasing the number of detectable analytes in the future, there may be many more possibilities to establish these sensors in root research (and elsewhere).

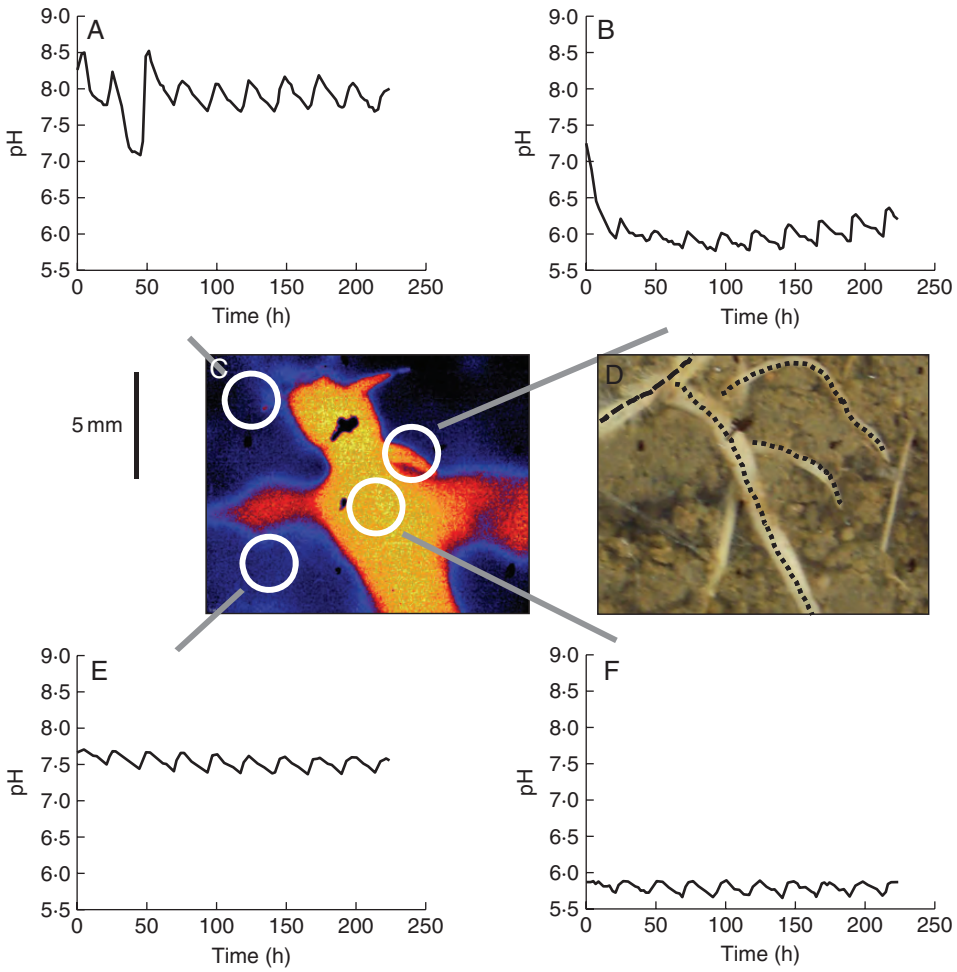


FIG. 4. (A–F) Line graphs displaying the diurnal pattern of pH values of selected areas around intercropped chickpea and wheat roots, taken from a 223-h pH monitoring (A = wheat root, B = basal part of chickpea lateral root, E = area without visible roots, F = chickpea root). White circles in the pH false colour map (C) indicate the corresponding source area for line graphs. Black lines in the photograph (D, taken at the end of the experiment) indicate roots that were grown during this phase of the experiment (dotted = chickpea; dashed = wheat). Other visible roots were grown in a later phase of the experiment. For additional images of pH dynamics we refer to the video sequence in Supplementary Data Video S3.

*Rhizosphere pH dynamics*

The pH monitoring of wheat and chickpea roots proved that this system is able to detect rapid pH changes in a very heterogeneous and dynamic microenvironment, a key feature of the rhizosphere, as stressed by, for example, Kim *et al.* (1999) and Walter *et al.* (2009). The necessity for high temporal and spatial monitoring systems becomes clear when dynamic processes such as the physiologically controlled diurnal rhythm of pH changes at the surface of the nodules on chickpea roots needs to be monitored. Chickpea roots and root nodules produce protons as $N_2$ fixation results in greater uptake of cations than anions. The $N_2$-fixing activity is an energy-costly metabolic process that requires the delivery of photosynthates to the bacteroids within the nodule, and might therefore be linked to the photosynthetic activity of the plant. Thus, photosynthesis during the day may sustain greater $N_2$ fixation than at night, and thereafter a greater acidification of the rhizosphere in the vicinity of $N_2$-fixing nodules along chickpea roots. A previous study had reported on such diurnal patterns of rhizosphere acidification in $N_2$-fixing legumes (Tang *et al.*, 2004), but the results were obtained at the whole root system level for hydroponically grown plants. The optodes enabled us to show that rhizosphere acidification and its diurnal pattern is especially clear in the vicinity of root nodules, which is in line with the recent observations made by Ding *et al.* (2012). However, these authors dealt only with the spatial, not temporal, dimension of this process.

Besides these diurnal processes around the nodules of chickpea, a second diurnal process along the roots of chickpea and wheat was detected. The diurnal pH dynamics were probably due to high pH of the water that was used for watering (pH 7·9). Hence, watering caused rapid dilution of the proton concentration, which then steadily increased again due to root activity. A temperature effect caused by the illumination can be ruled out, as the illumination of the chamber started 6 h prior to this effect and control pots showed no changes in soil temperature.

This study also revealed contrasting or even opposite behaviours for roots of different plant species. The wheat roots alkalized their rhizosphere, probably because of a large

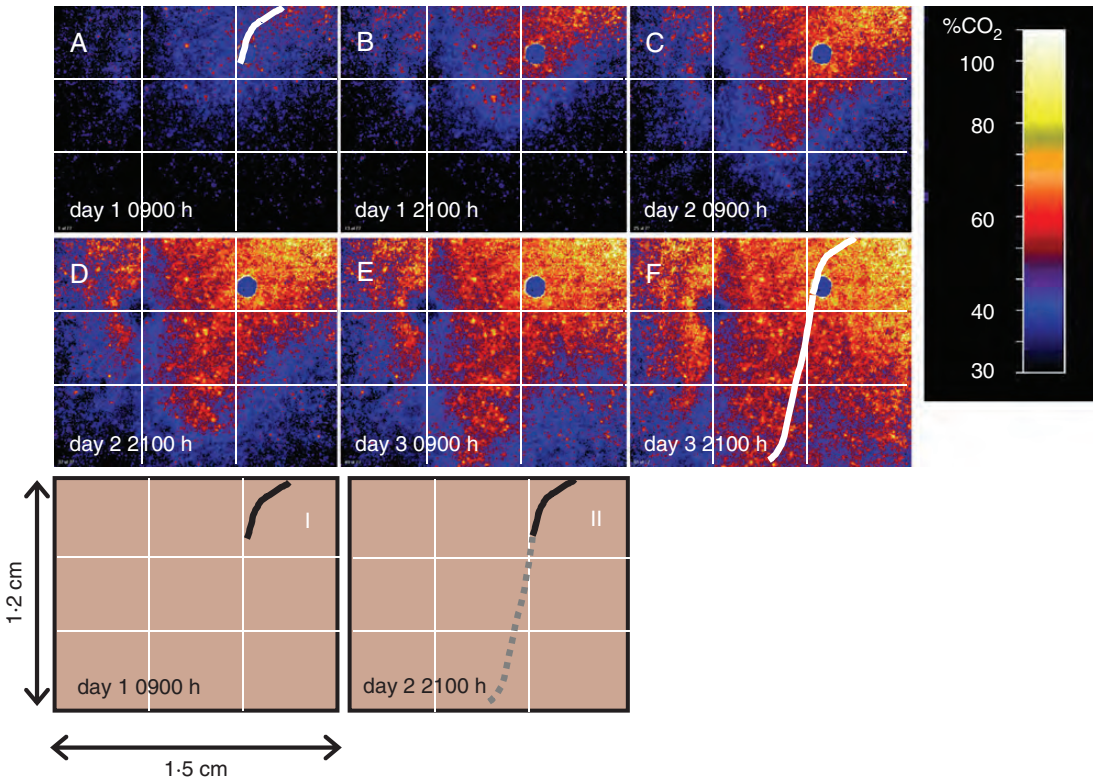


FIG. 5. (A–F) The six $CO_2$ maps display the dynamics of the $pCO_2$ around *V. juncea* roots, taken from a 76-h $pCO_2$ monitoring (white labelling indicates day of the experiment and hours of the day). White lines indicate the position of roots at the start and the end of the experiment. I and II: estimated position of the roots behind planar optode during the course of the experiment; the grey line indicates root growth compared with day 1 of the experiment. For additional images of $CO_2$ dynamics we refer to the video sequence in Supplementary Data Video S4.

nitrate uptake resulting in excess anion over cation uptake being counterbalanced by proton influx, and subsequent rhizosphere alkalization. This is extensively documented in the literature (e.g. Marschner and Römheld, 1983; Hinsinger *et al.*, 2003) and has been shown with the same species, cultivar and soil at the whole root system scale (e.g. Betencourt *et al.*, 2012). This alkalization was found to affect a large area (several $cm^3$) of the soil, as long as no other competing processes were taking place.

The added value of the optode technology is to show that prior to the massive alkalization of its rhizosphere, wheat roots exhibited an acidifying effect at their growing root tips, resulting in soil particles being significantly acidified prior to being alkalized to a greater extent, resulting ultimately in a net alkalization of the rhizosphere, as observed at the bulk level of the whole root system (Betencourt *et al.*, 2012). The root-induced acidification at the tip and in the elongation zone of wheat roots suggest greater uptake of cations than anions there, while the opposite was found in more mature zones of the roots. This effect is in good agreement with the acid growth mechanism (Mulkey and Evans, 1981; Weisenseel and Meyer, 1997; Peters, 2004). In contrast to wheat, chickpea roots extensively acidified their rhizosphere, even more so in the basal parts, presumably due to greater uptake of cations over anions in this legume, which relies on $N_2$-fixation as discussed above. This has been well documented although no previous studies have quantified the corresponding pH changes with such a spatial and temporal resolution. This is particularly relevant in the context of intercropping plant species with contrasted behaviours, as was achieved in the present experiment with wheat and chickpea. Raynaud *et al.* (2008) used theoretical models to address the interactions between neighbouring roots of two intercropped species exhibiting contrasting exudation patterns to understand the potential impact on the bioavailability of nutrients such as phosphate, and discuss plant–plant interactions in this context. They could not validate their findings experimentally due to the lack of proper technology. The optodes, as illustrated here in the case of intercropped wheat and chickpea, appear to provide a unique approach to fill this gap.

### *Rhizosphere $CO_2$ dynamics*

The imaging of $pCO_2$ around a growing root of *V. juncea* reported in the present work is the first to document the strong impact of a single growing root on the local $pCO_2$ over several millimetres within the soil. The high $pCO_2$ in the rhizosphere is probably not only due to the autotrophic respiratory activity of the root, but presumably also due to the heterotrophic activity of the microbial community that is growing as a biofilm on the root surface or as free-living organisms in the rhizosphere (collectively called rhizosphere respiration). However, to our knowledge, this kind of relationship has only been studied so far under non-saturated

conditions (Graham *et al.*, 2012). It is generally accepted that in a waterlogged substrate the $CO_2$ content can rise to such high levels, due to the hampered diffusion of $CO_2$ in water (Greenway *et al.*, 2006). Soils are also known to exhibit elevated $pCO_2$ compared with the atmosphere, due to restricted diffusion of $CO_2$ evolved from the respiration of roots and soil biota (Hinsinger *et al.*, 2009). However, until now an appropriate technique for non-invasive measurement of $CO_2$ in soils, at the spatial scale of hotspots of biological activities such as the rhizosphere, was lacking. The new $pCO_2$ optode system described in the present work fills this gap.

## CONCLUSIONS AND OUTLOOK

The present study proved this novel imaging system to be a powerful tool for monitoring and quantifying rhizosphere pH and $pCO_2$ dynamics at the sub-millimetre scale. By doing so, plant–plant and plant–soil interactions can be visualized clearly and measured quantitatively. The present system will pave the way for a better understanding of this environmental hot spot of plant and microbial activities, their temporal fate and spatial heterogeneity. However, to elucidate the wide range of bioprocesses in the rhizosphere, the monitoring of key environmental parameters alone is only a first step. Additionally, assessment of proton or $CO_2$ fluxes in the rhizosphere by means of digital image analysis tools would be the next step forward. A combination of this non-invasive optode technique together with other non- or minimally invasive (sampling) techniques should be the ultimate goal for detailed rhizosphere process mapping.

## SUPPLEMENTARY DATA

Supplementary data are available online at www.aob.oxfordjournals.org and consist of the following. Figure S1: the principle of sensor excitation by the camera system and the technical set-up. Figure S2: procedure for ratiometric image analysis. Figure S3: a typical calibration response of the pH sensor and the corresponding Boltzman fit for pH calculation. Figure S4: a typical calibration response of the $CO_2$ sensor and the corresponding Boltzman fit for $CO_2$ calculation. Video S1: dynamic patterns of pH around wheat roots from a 48-h monitoring period. Video S2: dynamic patterns of pH around chickpea nodules from a 48-h monitoring period. Video S3: dynamic patterns of pH around intercropped chickpea and wheat roots taken from 223-h monitoring. Video S4: dynamic patterns of $pCO_2$ around roots of *V. juncea* roots taken from a 76-h monitoring period.

## ACKNOWLEDGEMENTS

The financial support for French–German Scientific exchanges through the PROCOPE programme is gratefully acknowledged. S.B. received funding from the European Community Seventh Framework Programme FP7/2007-2013 (grant agreement no. 226532). C.M.S. was supported by the RHIZOPOLIS Grand Federative Project of Agropolis Fondation, Montpellier. Some other parts related to the implementation of the sensor systems were supported by the EURoot (Enhancing resource Uptake from Roots under stress in cereal crops) FP7-KBBE European project.

## LITERATURE CITED

**Betencourt E, Duputel M, Colomb B, Desclaux D, Hinsinger P. 2012.** Intercropping promotes the ability of durum wheat and chickpea to increase rhizosphere phosphorus availability in a low P soil. *Soil Biology and Biochemistry* **46**: 181–190.

**Blossfeld S, Gansert D. 2007.** A novel non-invasive optical method for quantitative visualization of pH-dynamics in the rhizosphere of plants. *Plant, Cell & Environment* **30**: 176–186.

**Blossfeld S, Perriguey J, Sterckeman T, Morel J-L, Loesch R. 2010.** Rhizosphere pH dynamics in trace-metal-contaminated soils, monitored with planar pH optodes. *Plant and Soil* **330**: 173–184.

**Blossfeld S, Gansert D, Thiele B, Kuhn AJ, Lösch R. 2011.** The dynamics of oxygen concentration, pH value, and organic acids in the rhizosphere of *Juncus* spp. *Soil Biology and Biochemistry* **43**: 1186–1197.

**Bravin MN, Tentscher P, Rose J, Hinsinger P. 2009.** Rhizosphere pH gradient controls copper availability in a strongly acidic soil. *Environmental Science and Technology* **43**: 5686–5691.

**Ding XD, Sui XH, Wang F, *et al*. 2012.** Synergistic interactions between *Glomus mosseae* and *Bradyrhizobium japonicum* in enhancing proton release from nodules and hyphae. *Mycorrhiza* **22**: 51–58.

**Graham SL, Millard P, Hunt JE, Rogers GND, Whitehard D. 2012.** Roots affect the response of heterotrophic soil respiration to temperature in tussock grass microcosms. *Annals of Botany* **110**: 253–258.

**Greenway H, Armstrong W, Colmer TD. 2006.** Conditions leading to high $CO_2$ (>5 kPa) in waterlogged-flooded soils and possible effects on root growth and metabolism. *Annals of Botany* **98**: 9–32.

**Gansert D, Blossfeld S. 2008.** The application of novel optical sensors (optodes) in experimental plant ecology. In: Lüttge U, Beyschlag W, Murata J. eds. *Progress in botany.* Berlin: Springer, 333–358.

**Gollany HT, Schumacher TE, Rue RR, Liu S-Y. 1993.** A carbon dioxide microelectrode for *in situ* $pCO_2$ measurement. *Microchemistry Journal* **48**: 42–49.

**Hiltner L. 1904.** Über neuere Erfahrungen und Probleme auf dem Gebiet der Bodenbakteriologie und unter besonderer Berücksichtigung der Gründüngung und Brache. *Arbeiten der Deutschen Landwirtschaftlichen Gesellschaft* **98**: 59–78.

**Hinsinger P, Plassard C, Tang CX, Jaillard B. 2003.** Origins of root-mediated pH changes in the rhizosphere and their responses to environmental constraints: a review. *Plant and Soil* **248**: 43–59.

**Hinsinger P, Gobran GR, Gregory PJ, Wenzel WW. 2005.** Rhizosphere geometry and heterogeneity arising from root-mediated physical and chemical processes. *New Phytologist* **168**: 293–303.

**Hinsinger P, Bengough AG, Vetterlein D, Young IM. 2009.** Rhizosphere: biophysics, biogeochemistry and ecological relevance. *Plant and Soil* **321**: 117–152.

**Holst G, Grunwald B. 2001.** Luminescence lifetime imaging with transparent oxygen optodes. *Sensors and Actuators B: Chemical* **74**: 78–90.

**Kim TK, Silk WK, Cheer AY. 1999.** A mathematical model for pH patterns in the rhizosphere of growth zones. *Plant Cell and Environment* **22**: 1527–1538.

**Marschner H, Römheld V. 1983.** *In vivo* measurement of root-induced pH changes at the soil–root interface: effect of plant species and nitrogen source. *Zeitschrift für Pflanzenernährung und Bodenkunde* **111**: 241–251.

**Mulkey TL, Evans ML. 1981.** Geotropism in corn roots: evidence for its mediation by differential acid efflux. *Science* **212**: 70–71.

**Neumann G, George TS, Plassard C. 2009.** Strategies and methods for studying the rhizosphere – the plant science toolbox. *Plant and Soil* **321**: 431–456.

**Ott T, van Dongen JT, Gunther C, *et al*. 2005.** Symbiotic leghemoglobins are crucial for nitrogen fixation in legume root nodules but not for general plant growth and development. *Current Biology* **15**: 531–535.

**Peters WS. 2004.** Growth rate gradients and extracellular pH in roots: how to control an explosion. *New Phytologist* **162**: 571–574.

**Raven JA, Franco AA, Dejesus EL, Jacobneto J. 1990.** $H^+$ extrusion and organic-acid synthesis in $N_2$-fixing symbioses involving vascular plants. *New Phytologist* **114**: 369–389.

**Raynaud X, Jaillard B, Leadley PW. 2008.** Plants may alter competition by modifying nutrient bioavailability in rhizosphere: a modeling approach. *American Naturalist* **171**: 44–58.

**Rudolph N, Esser HG, Carminati A, *et al*. 2012.** Dynamic oxygen mapping in the root zone by fluorescence dye imaging combined with neutron radiography. *Journal of Soils and Sediments* **12**: 63–74.

**Schreiber CM, Zeng B, Blossfeld S, *et al*. 2012.** Monitoring rhizospheric pH, oxygen and organic acid dynamics in two short-time flooded plant species. *Journal of Plant Nutrition and Soil Science* **175**: 761–768.

**Tang C, Drevon JJ, Jaillard B, Souche G, Hinsinger P. 2004.** Proton release of two genotypes of bean (*Phaseolus vulgaris* L.) as affected by N nutrition and P deficiency. *Plant and Soil* **260**: 59–68.

**Walter A, Silk WK, Schurr U. 2009.** Environmental effects on spatial and temporal patterns of leaf and root growth. *Annual Review of Plant Biology* **60**: 279–304.

**Watt M, Silk WK, Passioura JB. 2006.** Rates of root and organism growth, soil conditions, and temporal and spatial development of the rhizosphere. *Annals of Botany* **97**: 839–855.

**Weisenseel MH, Meyer AJ. 1997.** Bioelectricity, gravity and plants. *Planta* **203**: 98–106.